

OPTIMIZATION OF THE DETECTION SYSTEM FOR ^{16}N REGISTRATION ALONG WITH COOLANT LEAKS IN THE WWER-1000 STEAM GENERATOR

V.G. Rudychev¹, Y.V. Rudychev^{2}, N.A. Azarenkov¹, A.Y. Bondar¹*

¹ *Kharkov National University, Kharkov, Ukraine;*

² *National Science Center "Kharkov Institute of Physics and Technology", 61108, Kharkov, Ukraine*

(Received April 17, 2013)

One of the methods of control of steam generator coolant flow from the primary circuit to the 2nd circuit is a measurement of the isotope ^{16}N activity. Aim of this work is the optimizing of characteristics and placements of NaI(Tl) detectors. Radiation transport from steam-line volume to the detector by Monte-Carlo method is simulated using MCNP and PENELOPE packages. The special procedure, which can decrease a simulation time due to increasing numbers of "virtual detectors" arranged around steam-line irradiation source, is developed. Influence of the NaI detector thickness to the amount of absorbed photons, which ones characterized ^{16}N evidence, co-called response function is investigated. Different variants of cylindrical detectors with constant volume, which have various diameter to the height ratios is investigated. Arrangement of ones around steam-line irradiation source is optimized.

PACS: 28.41.Qb, 28.41.Ak, 28.41.Fr, 28.31.Te, 24.10.Lx, 29.30.Kv,

1. INTRODUCTION

One of the possible accidents in the operation of WWER-1000 is a steam generator coolant flow from the primary circuit to the 2nd circuit. The extent of the accident is determined by the level of leakage. With low flow of coolant the radioactive contamination of pipelines and turbines occurs. At high levels of leakage a large-scale accident becomes more probable. Due to the large pressure difference (in the 1st circuit 160 atm, and in the 2nd 60 atm) the possibility of the steam-line second circuit rupture appears. The ejection of radioactive coolant under containment or into the atmosphere becomes possible. When the leakage rate is low only the turbine contamination occurs. One of coolant leak control methods is to use a radiometric method based on measuring the activity of the isotope ^{16}N in the steam out of containment. Many firms [1],[2],[3] offer ^{16}N activity measurement systems based on scintillation detectors with crystals NaI (Tl). The existing designs, as well as the available literature, has no data about the optimal of proposed installations for level of ^{16}N activity measurement.

The purpose of this work is to determine radiation fields around the steam-lines and to optimize characteristics of the detection system and its arrangement.

2. INITIAL DATA

The radioactivity of the primary circuit coolant is determined by:

- Self-radioactivity; - Impurity radioactivity; - Radioactive due to leaks from fuel cladding.

The coolant self-radioactivity is due to neutron activation of nuclear elements that are part of the coolant. The determining source of the coolant self-activity for WWER-1000 reactor is a radioactive isotope of nitrogen ^{16}N with a half-life of 7.12 seconds. This isotope of nitrogen is generated by irradiation with high-energy neutrons of the oxygen isotope ^{16}O in the following reaction:



It should be noted that content of the isotope ^{16}O in natural elements (oxygen) is 99.76% coolant radioactivity is determined by activation of corrosion and erosion products of metal structures through which the coolant flows, as well as by natural impurities. Radioactivity induced by leakage of fuel cladding is due to leaching of fuel fission products and actinides. Decrease of the impurity radioactivity as well as the activity induced by fuel cladding leaking can be reached by cleaning of the coolant.

It is known that the coolant self-activity in the WWER-1000 exceeds both the impurity activity and that induced by the fission products and actinides in ≈ 1000 times. Formation reaction of $^{16}\text{O}(n, p)^{16}\text{N}$, is the threshold reaction. The formation of ^{16}N begins with neutron energy $E_{lev} = 10.24452 \text{ MeV}$ [4] To make correct calculation of the output of nitrogen 16 for different reactor operation modes is quite difficult. Such calculations, in which changes of the neutron spectrum in the slowing process, and the design features of pressurized water reactors WWER-1000 are taken into account, can be performed using, for ex-

*Corresponding author E-mail address: rudychev@kipt.kharkov.ua

ample, package ORIGEN [5]. A detailed study of the formation of ^{16}N is not the purpose of this work. And to estimate the formation of ^{16}N we use the following simplified scheme: the output of ^{16}N is proportional to the high-energy component of the fission spectrum of ^{235}U and the corresponding cross section $\sigma(E)$ of the reaction $^{16}\text{O}(n, p)^{16}\text{N}$, as well as the total flux of neutrons in the reactor. Then the number of ^{16}N atoms will be determined by the following relation:

$$f_{16} = \left(\frac{N_{O16} \cdot N_n}{E_{max} - E_{min}} \right) \cdot \int_{E_{lev}}^{E_{max}} \sigma(E) \cdot \chi(E) dE, \quad (2)$$

where N_{O16} is the number of oxygen 16 atoms in cubic cm of coolant, N_n is the neutron flux in the coolant per square cm, E_{lev} is a neutron threshold energy for formation of ^{16}N , $\chi(E)$ is the spectral distribution of the ^{235}U fission neutrons. Neutron spectrum $\chi(E)$ is calculated by the formula of Watt, which has the following form for the different energy ranges:

$$\chi(E) = 0.4839 \cdot \exp(-E) \cdot \sinh(\sqrt{2E}) \cdot f_I(E), \quad (3)$$

where $f_1 = 0.913 + 0.75 \cdot E$ for $0.01 < E \leq 0.25$,
 $f_2 = 0.944 + 0.0644 \cdot E^{-0.608}$ for $0.25 < E \leq 10$,
 $f_3 = 2.94 \cdot \exp(11.3/E)$ for $10 < E \leq E_{max}$.

Fig.1 shows the dependences of the cross sections of the reaction $^{16}\text{O}(n, p)^{16}\text{N}$ from the incident neutron energy and the evaluated data ENDF / B-VI from the library [4]. The figure also shows the high-energy part of the neutron fission spectrum of ^{235}U with a factor 10^2 [6],[7]. The mentioned data indicate that the cross section of ^{16}N formation decreases slowly with increasing the neutron energy. Note that for neutron energies above 17 MeV their number is rather small $< 10^{-5}$, this is with area spectrum normalization, i.e. integral taken through spectrum = 1. So we take the maximum energy value in relation (2) $E_{max}=18\text{MeV}$. Then the number of neutrons in the energy range $E_{lev} < E \leq E_{max}$ is $\approx 10^{-3}$ of the total number of neutrons.

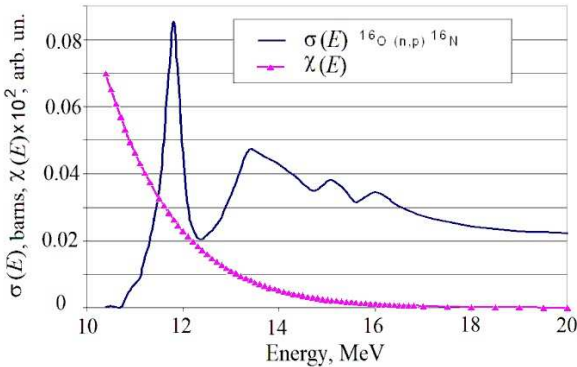


Fig.1. Dependences of ^{16}N formation cross-section and number of incident neutrons from energy

Table 1. Emission characteristics of ^{16}N

Energy, Mev	1.75	1.95	2.74	6.13	6.92	7.12	8.87
Radiation yield per 1 decay	1.30E-03	4.20E-04	7.60E-03	6.90E-01	4.20E-04	5.00E-02	7.00E-04
Percentage per 1 photons, %	0.17	0.06	1.01	91.95	0.06	6.66	0.09

Fig.2 shows the dependence of the product of ^{16}N cross section and the neutron flux of given energy, which is proportional to the activation of the isotope ^{16}O as a function of energy. Note that the area under this curve is called activation integral.

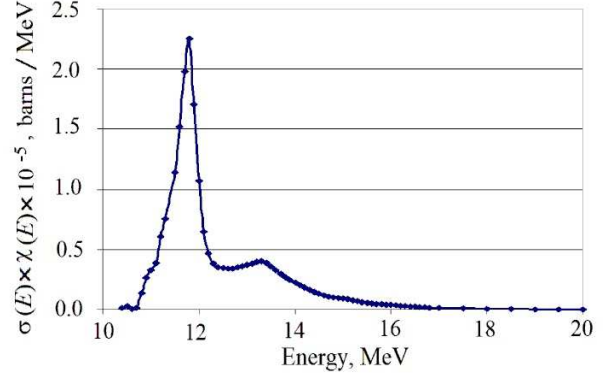


Fig.2. Dependence of $\sigma(E) \times \chi(E)$ from neutrons energies

During operation of the WWER-1000 reactor at nominal mode (3-year company), the average flux of neutrons $N_n \approx 3.8 \cdot 10^{14}$ per cm^2 . [7] With an average coolant temperature of 330 and a pressure of 160 kg/cm^2 coolant density is $0.7 \text{g}/\text{cm}^3$. With these conditions, the number of oxygen 16 atoms in cm^3 $N_{O16} = 2.34 \cdot 10^{22}$. Using reaction (2) and the data from Fig.2 we can get the estimation of Nitrogen 16 activity in the coolant during reactor operation at nominal power of 3000 MW thermal power:

$Q_{N16} = 2.60 \cdot 10^9 \cdot (\text{Bk}/\text{kg})$ From the data presented in the literature [9] ^{16}N activity reaches up to $3.7 \cdot 10 \cdot 10^9$ and even $7.6 \cdot 10 \cdot 10^9$ Bk/kg.

Comparing the data on the activity of corrosion and activation products as well as the activity of fission products and actinides [9] and coolant self-activity (by Nitrogen 16) it follows that the activity of ^{16}N is several times higher than that of all the rest radionuclides in coolant.

^{16}N is a radionuclide with a half-life time $T_{1/2} = 7.12$ s, with a high yield of high-energy gamma rays [4]. Table 1 shows the quantum yields of gamma rays with different energies per 1 decay and the partial contribution of gamma-quanta with different energies.

3. MODELING OF THE SOURCE AND THE DETECTING SYSTEM

Steam generators of PGW-1000 type are used in the WWER-1000 reactors. These steam generators are part of the circulation loop and are designed to produce the vapor with pressure of 6.27 MPa (64 kgf/cm²) with a humidity of 0.2% at 279,5. 1470 tons of feedwater is evaporated and 44 290 m³ ($\approx 4,42 \cdot 10^4$) of steam per hour is produced in the steam generator. Obviously, that due to leakage of the coolant of first circuit up to several tons per hour the steam capacity remains almost unchanged. Even addition of 2.5 tons of coolant to 1470 tons of feedwater is about 0.15%. However, the volume of produced steam contains all the radionuclides contained in the leaked coolant. Concentration of ¹⁶N in the vapor will be determined both by the initial concentration of ¹⁶N in the coolant and by the decrease due to coolant travel time to the steam generator and travel time of steam to the detection system. In this paper changes in the activity of ¹⁶N due to moving of steam and coolant to the detection system are not studied.

Determination of ¹⁶N concentration in the 2nd circuit steam-line is performed outside the reactor section, i.e. outside hermetic containment. This is accounted for by the fact that the steam generators and pipelines of the 1st circuit are powerful radiation sources, because they are filled with coolant with highly concentrated ¹⁶N. Both hermetic containment (thickness of reinforced concrete 1.2 m), and rather large distance from the steam generators and pipelines of 1st circuit serve as radiation protection of the detection system. Let us examine the conditions of a radiation field formation in the presence of ¹⁶N in the steam. We use a number of methods for calculation of the source-induced radiation field and for determination of the gamma-ray flux entering the detector:

- Monte Carlo method, modeling a source of ra-

$$N_\gamma(b, h, E) = \frac{n_\gamma(E)}{2\pi} \int_0^h dz \int_0^R \rho d\rho \int_0^\pi \frac{B_1(\mu(E)t_1 x/R) \cdot B_2(\mu_2(E)t_2 x/R) e^{-(t_1 \cdot \mu_1(E) + t_2 \cdot \mu_2(E)) \cdot \frac{x}{R}} d\phi}{\rho^2 + b^2 + z^2 - 2b\rho \cos(\phi)}, \quad (4)$$

where $x = x(z, \rho, \phi)$ is the distance from the point volume to the cylinder lateral surface, b is the distance from the axis of the cylinder to the point of observation P, R - radius of the cylinder, h - height of the cylinder, t1 - thickness of the cylinder steel walls, $\mu_1(E)$ - linear attenuation coefficient of the walls ma-

$$x = \frac{\rho^2 - b\rho \cos \phi + \sqrt{(\rho^2 + b^2 - 2b\rho \cos \phi)R^2 - \rho^2 b^2 \sin^2 \phi}}{\rho^2 + b^2 - 2b \cos \phi} \sqrt{\rho^2 + b^2 + z^2 - 2b\rho \cos \phi}. \quad (5)$$

For the case when the observation point P is located at the height h_z from the source base, relation for radiation flux is as follows:

$$Nh_\gamma(b, h_z, E) = N_\gamma(b, h_z, E) + N_\gamma(b, h - h_z, E) \quad (6)$$

diation and detection system - packages PENELOPE and MCNP [11];

- The method of volume integration of point light sources arranged in a cylindrical volume [12];

Modern packages (PENELOPE and MCNP), based on the Monte Carlo gives comprehensive information about the transport of radiation for complex geometric configurations, both the source and detection systems. However, these methods require very long calculations. Method of volume integration of point sources is quite effective for a number of tasks.

Emitting steam-line is a volume cylindrical source with steel walls covered with heat-insulation. It is assumed that each element of the source volume dV isotropically emits gamma rays with energy E and density $n_\gamma(E)$.

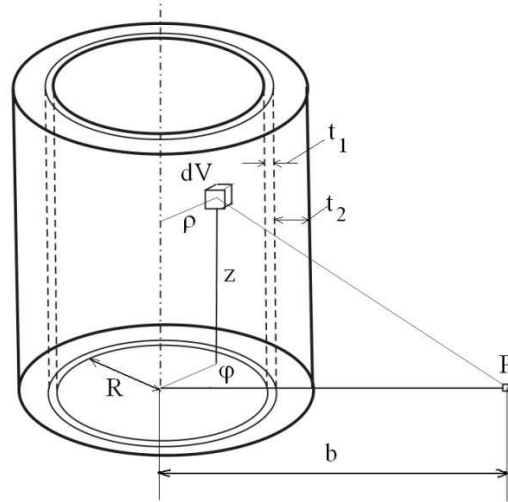


Fig.3. Geometry for cylindrical volume source without protection

Then the amount of gamma-quanta N_γ in the radial direction at the point P (see Fig.3) located in the base plane of the source, can be written as:

terial, B1 - build-up factor in the iron for a point source, t2 - insulation thickness, $\mu_2(E)$ - the linear attenuation coefficient of the insulation material, B2 - build-up factor in the heat-insulation for a point source. The expression $x = x(z, \rho, \phi)$ The expression for $x(z, \rho, \phi)$ is as follows:

Relation (4) differs from the commonly used [12] In this relation self-absorption in the source volume is not taken into consideration, but the absorption in the steel walls and in the heat-insulation of steam-

line is. The absorption of gamma rays in steam-line is almost absent because of the low density of steam in the pipe $\rho \approx 0.03 \text{ g/cm}^3$. Steam pipe of live steam is the pipe with an outside diameter of 63 cm and a wall thickness of 25 mm [2], made of austenitic steel. Pipe is covered with insulation with density of 0.15 g/cm^3 made of SiO_2 and 10 cm thick. [1] To solve the problem a mathematical model was developed to simulate the pipeline - detector system. Geometry of the detector system and pipeline is visualized in package MCNP and is shown in Fig. 4, and the model in package PENELOPE is shown in Fig. 5.

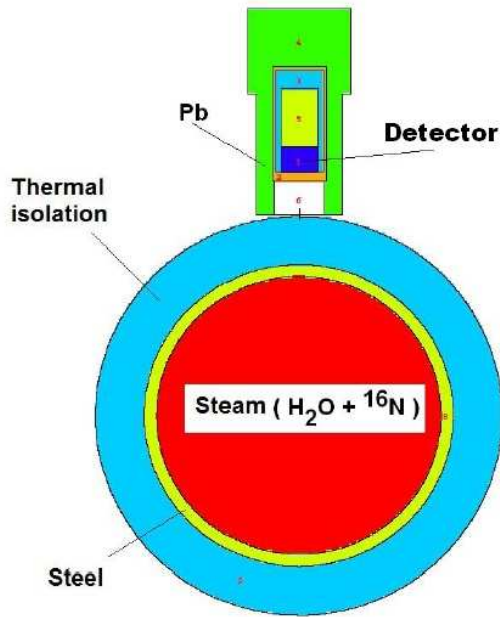


Fig. 4. Geometry of detecting system and pipeline in the package MCNP visualization

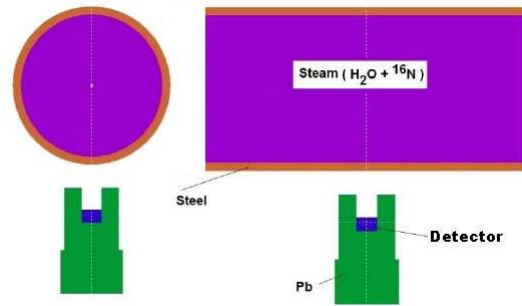


Fig. 5. Geometry of detecting system and pipeline in the package PENELOPE visualization

The geometric models presented above were used to determine gamma-ray flux in the detector from a segment of steam-pipe filled with steam containing ^{16}N using the Monte Carlo methods. Throughout the whole volume of the steam-pipe gamma rays from the decay of ^{16}N (see Table 1) were generated and distributed isotropically in all directions. We took into account only the photons that reached the detector volume. Some versions of lay-out both for the detection systems in a shielded box of lead (collimator) and for those without shielding were considered. Geometry of the source and the detector (Figs. 4 and 5) shows that the detector gets a small fraction of gamma rays produced in the steam-pipe.

Traditional methods of particle transport calculation with Monte Carlo methods are very time-consuming for obtaining statistically reliable results. In connection with this registration methods using "ring", "spherical" or "point", "detector" [11] are employed. Such approaches can significantly decrease the calculation time. We have proposed an alternative approach compared to the "ring" detectors. While simulating the emitter-detector system several "virtual" detectors shown in Figs. 4 and 5 were used. Fig. 6 shows the simulation variants of multiple detector systems arrangement around the steam-pipe both in packages MCNP and PENELOPE.

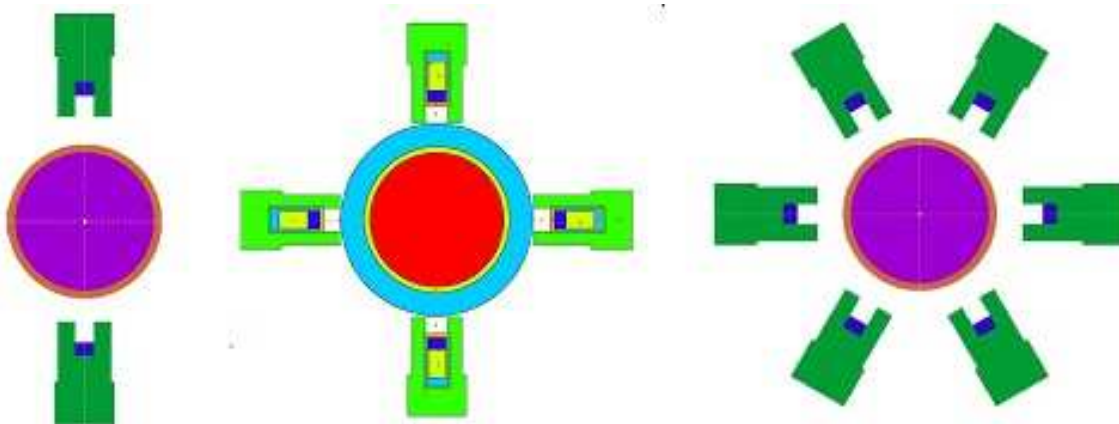


Fig. 6. Both detection system and steam-line geometry visualization in packages PENELOPE and MCNP

In calculations of radiation transport using Monte Carlo method the calculation time significantly depends on the geometry complexity and the multiplicity of materials used (elemental composition) in the objects to be simulated. We considered two variants of the detection system: the detector is placed in a shielded box of lead (collimator) and without screening unit. The detector was simulated to have a cylindrical volume with a diameter of 3 "and height of 2", the wall thickness of the lead collimator of 5 cm.

Fig. 7 shows the event generation rate for detecting systems depending on the number of detection units placed around the emitting steam-pipe. From the data in the figure it is obvious that in a system without a collimator the event registration speed in the "detector" is almost directly proportional to the quantity of the recording "detectors". Calculation speed slows when the detection system is complicated. In the presence of a collimator for 8 detectors the computation speed increases ≈ 6.2 times.

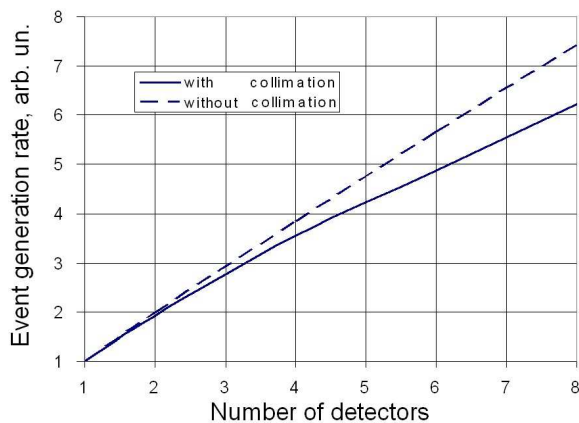


Fig. 7. Event generation rates depending on the number of the detecting units in the detecting systems without collimation and with collimation

4. CHARACTERISTICS OF THE RADIATION FIELD FROM STEAM-LINE

In our case, the radiation source is a cylindrical volume with radius of 29 cm, filled with low density steam ($\rho \approx 0.03 \text{ g/cm}^3$) containing ^{16}N . It was put in the steel pipe with an external diameter of 63 cm covered with heat-insulation with thickness of 10 cm. Because of the low density of the inside volume emitting gamma-quanta, self-absorption almost lacks in it, as well as actually there is no absorption in the heat-insulation, due to its low density ($\rho \approx 0.15 \text{ g/cm}^3$). The steam pipe goes out from the reactor hermetic containment area to the rigging premise and goes further into the turbine section. Therefore, to be specific, we take a 3 m long segment of a radiating pipe. It is known that radiation of a cylindrical source with a limited height (in our case, the height=3 m) decreases with distance along the radius and has its maximum at mid-height [13].

Calculations of gamma-ray flux for this steam-pipe were performed using relations (4)-(6). In Figure 8 the gamma-ray flux intensities along the steam line

at various distances are given. Curves: 1 - intensity of gamma-ray flux on the surface of heat-insulation, 2 and 3 - at distances of 5 and 10 cm from the surface of the insulation. Note, that at the distance of 10 cm from the surface of the insulation the decrease of the intensity of gamma ray flux exceeds 25%.

The guideline of the ^{16}N detection systems designers to place the detectors as close to sinking in the heat-containment as possible is well known. It is accounted for the fact that while transporting ^{16}N along the steam-line the activity is decreased because of the short half-life time of the isotope. Let us assume that the detectors are placed at a distance of 0.25 m from the sinking and at a distance of 1.5 m (i.e., across the center of the considered steam-line). Then, from the data given in Figure 8, it follows that the flux of gamma rays in the detector, placed in the center of steam, increases by 21, 23 and 25% in comparison with the same detector placed at the edge. At a steam rate in a steamline = 47 m / s. The time of ^{16}N passage is $1.25 \text{ m} / 47 \text{ m} / \text{s} = 0.0266 \text{ s}$. ^{16}N activity decay during this period is determined by: $\exp(-0.693 \times 0.0266 \text{ s} / 7.12\text{s}) = 0.997$, i.e. $\approx 0.3\%$. Thus, the efficiency of the radiation detection will be higher when the detection system is arranged across the center of the steam-line.

An important feature of the radiation is its spectral composition, which significantly determines the efficiency of detection. ^{16}N emits two main lines with energies of 6.13 and 7.12 MeV. The absorption of gamma rays having such energies is minimal for almost all materials. For iron (steam wall) the absorption coefficient of gamma rays due to the photoelectric effect is less than 1% of the total absorption coefficient. Tab. 2 shows the mass absorption coefficient of gamma rays in iron.

Table 2. The mass absorption coefficient of gamma rays in iron

Energy	Absorption coefficients			
	Photo	Compt	Pair	Tot
6.13	2.14E-05	2.03E-02	1.02E-02	3.05E-02
7.15	1.77E-05	1.83E-02	1.18E-02	3.01E-02

The transformation of the spectral composition from the volume of steam-pipe through the steel walls in a detection system that is located across the steam center due to the photoelectric effect and pair production is shown in Fig. 9. The presented results for the real geometry of the emitter were obtained using packages MCNP and PENELOPE. In comparison with the initial spectrum of ^{16}N , rather a large number of gamma rays at low energies appear. Annihilation peak 0.511 MeV is rather good observed, though absorption of pairs 2 times is less intensive than photoelectric effect.

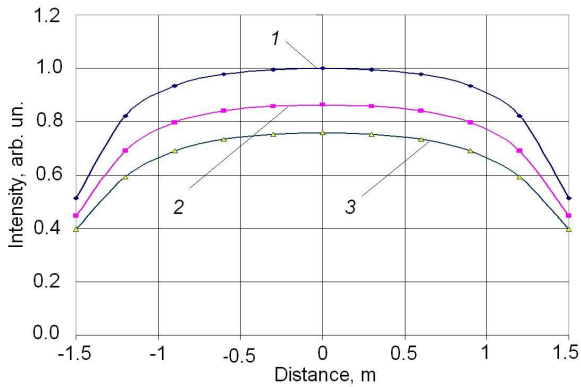


Fig. 8. Intensities of gamma-quanta along the steam-line on different distances. 1- at the surface of the insulation, 2 and 3- on distances 5 and 10 cm from the surface of the insulation

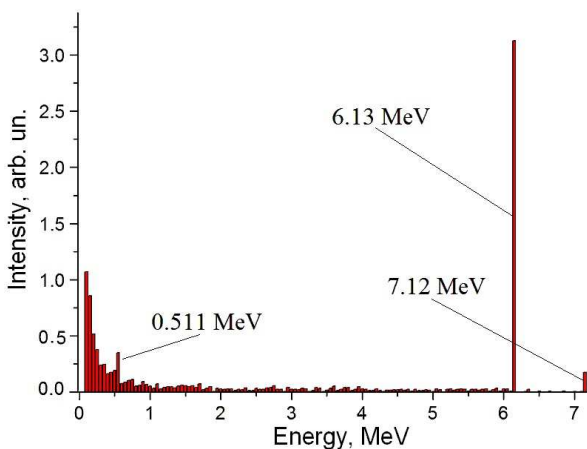


Fig. 9. A steam-line filled with the steam with ^{16}N covered with steel wall radiation spectral distribution

5. THE DETECTION SYSTEM

Nowadays scintillation methods are most commonly used for spectrometric research of gamma radiation. Inorganic crystals, that can have a large volume, are widely used as scintillators. Such crystals provide sufficiently high sensitivity of detection and measurement of gamma-rays within a wide range of energies. Such crystals as NaI (Tl) are used most widely. For these crystals methods of growth, allowing to get samples of large size and high transparency are developed. Recently developed heavy oxide crystals $\text{Bi}_4\text{Ge}_3\text{O}_{12}$ CdWO_4 have greater efficiency of high-energy radiation registration (per 1 cm^3 of volume), but their size is much smaller and as to their overall (total) efficiency they are inferior to the detectors based on crystals of NaI (Tl).

The available literature has no data about characteristics of scintillation detectors based on crystals NaI (Tl) for carrying out measurement the gamma-rays with energies above 4 MeV. For example, spectrometric characteristics of cylindrical crystals NaI (Tl) are given for different values of diameter and height for energies 0.662, 1.275 and 2.61 MeV

[14]. Although there are some examples of large crystals usage for registration of high-energy γ -rays [1]. Optimization of spectral characteristics of NaI (Tl) crystals such as light yield and optical absorption, proper and total resolution, etc is not the objective of our research.

The objectives of our research are: to determine the relationship between the diameter and height, with the possible limitation of the detector volume, as well as to determine the arrangement of the detector relative to the steam-line aiming to achieve the most effective absorption of high-energy gamma-rays from ^{16}N .

The total absorption coefficient of gamma rays for NaI (Tl) is a bit ($\sim 15\%$) higher than that for the iron due to the larger atomic number of iodine. Absorption owing to the Compton effect is practically equal to the absorption caused by to the pair production. Table 3 shows mass absorption coefficients of gamma rays in NaI (Tl).

Table 3. The mass absorption coefficients of gamma rays in NaI (Tl)

Energy	Absorption coefficients			
	Photo	Compt	Pair	Tot
6.13	1.95E-04	1.86E-02	1.61E-02	3.48E-02
7.15	1.61E-04	1.67E-02	1.84E-02	3.53E-02

The computation of changes in the radiation spectrum from the steam-line in a detection system having a NaI $3'' \times 2''$ (just crystals with such dimensions are suggested to be used [1]) located across the steam-line center was performed. The spectra for real geometry of the radiator are computed using packages MCNP and PENELOPE and are shown in Fig. 10. Owing to significant contribution of the electron-positron pairs born with such energy into the process of photon absorption the annihilation peak of 0.511 MeV dramatically increases. In comparison with the spectrum of photons from the steam-line, gamma-ray photons with low energy (energy is less than 0.511 MeV) are absorbed more effectively in NaI than in iron, which is shown in Fig. 10.

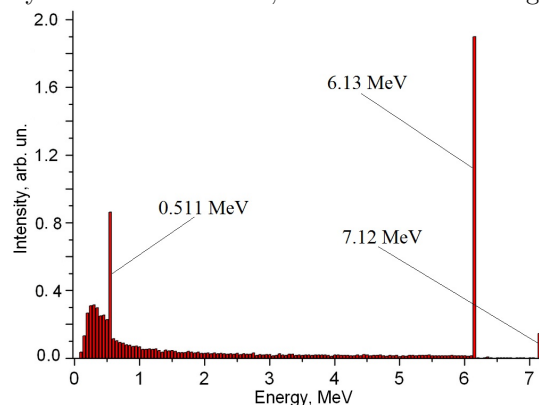


Fig. 10. Steamline radiation spectra transformation in the detector NaI(Tl)

Comparison of the spectra in Fig.9 and Fig.10 shows a significant decrease in the intensity of high-energy initial lines (6.13 and 7.12 MeV) in the detector with the dimensions: diameter = 3" and height = 2". Change in the intensity of the main lines in the detector actually determines efficiency of gamma ray flux detection.

To simulate the detection of ^{16}N gamma radiation with scintillation detector based on NaI crystal the packages MCNP and PENELOPE were used. To determine the function of the detector response Pulse Height Tallies distribution was used [11]. In fact, this distribution is similar to the physical detector. The energy intervals of our distribution correspond to the total emitted energy in a given channel for each physical particle, unlike other distributions that characterize the track energy in a predetermined energy range. Modeling using Monte Carlo simulation (in packets MCNP and PENELOPE) allows to obtain the distribution of the absorbed energy (deposited energy) - the response function of NaI detector. This distribution is an ideal approximation of the signal measured by a real instrument. In fact, there is a "smearing" of the signal because of not 100% efficiency of charge collection and of various losses in an electronic unit and photomultiplier.

As a rule, for the registration of high-energy γ -quanta the total absorbed energy is determined (deposited energy - response function) in the energy range $(0.75...1.0) \cdot E_{\text{max}}$, where E_{max} is the maximum energy of the photons.

In our case 91% of the ^{16}N radiation has an energy 6.13 MeV. Radiation length of this energy in the NaI (exponential attenuation of the radiation by e times) $= 1/\mu_{\text{tot}}(6.13) = 7.83$ cm. Just γ -quanta absorbed in the detector will determine the effectiveness of registration. Obviously, the number of caught gamma rays (for parallel beam) for a cylindrical detector is proportional to its area (diameter), and the extent of absorption is proportional to the height of the cylinder accounting for the edge effects.

Let's examine the effect of the height of NaI detector on the efficiency of photon detection. To simplify the model we regard a NaI detector as infinite plates of different thicknesses, on which γ -quanta with the energy of 6.13 MeV normally fall. The effectiveness of the registration $N_{\text{eff}}^{\text{slab}}$ is defined as the sum of the absorbed energies (deposited energy) in the detector at the energy range of γ -quanta 4.5...6.13 MeV. 5 cm layer of sodium iodide absorb $\approx 47\%$ γ -ray. For definiteness, we assume $N_{\text{eff}}^{\text{slab}}(5) = 1$ for a NaI layer thickness = 5 cm (≈ 2 inches). Dependence of $N_{\text{eff}}^{\text{slab}}$ from NaI thickness (curve 1) shown in Fig. 11. This figure also shows the dependence of the absorption of γ -quanta in the exponential approximation Kg (curve 2). Kg is defined by the following relation:

$$Kg = (1 - e^{(\mu_{\text{tot}}(6.13) \cdot t)}) / (1 - e^{(\mu_{\text{tot}}(6.13)) \cdot 5}), \quad (7)$$

where t is a layer thickness in *cm*. Data shown on Fig.11 illustrate the well-known fact that for the registration of high-energy γ -rays detectors must be large, i.e. with the thickness of 3...4 inches

[15],[16]. Indeed, doubling the thickness of the NaI from 5 cm to 10 significantly increases the efficiency of detection of γ -rays with energies of 6.13 MeV.

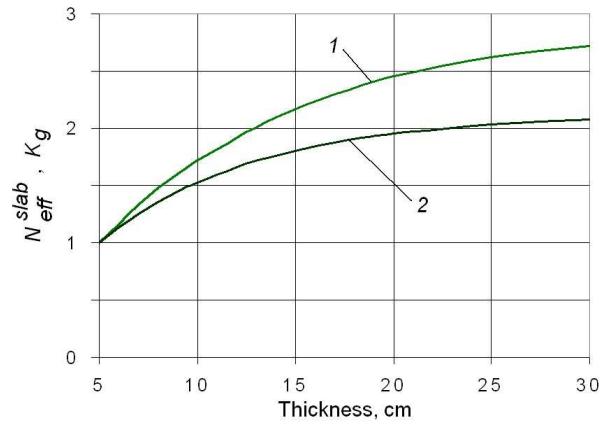


Fig.11. The dependence of registration efficiency (1) and γ -quanta absorption (2) from the thickness of the NaI layer

Note that for isotropic photons falling on the plate model detection efficiency increases by about 10% (for a part of γ -rays that fall on the plate at angles other than 90 degrees), path length increases. In accordance with the scheme shown in Figures 4 and 5 for the detection system and piping in packages MCNP and PENELOPE calculations are performed for response function in detector with crystal NaI 3" \times 2" without collimator. Fig.12 shows the response function (deposited energy) for the simulation of gamma radiation isotope ^{16}N . Energy range (4.5...7.2 MeV), which actually determines N_{eff} - radiation detection efficiency of nitrogen 16 is chosen.

Using the technique of virtual detectors in geometry (Figs. 4, 5) made it possible to determine the detection efficiency with accuracy better than 5%. The efficiency of detection without the collimator is $5.7 \cdot 10^{-5}$ pulse per one source γ -quanta.

The efficiency of detection with lead collimator with a thickness of 5 cm (see Fig. 4) is $2.7 \cdot 10^{-5}$ pulse per one source γ -quanta. Appearance of the response function in such system insignificantly differs from the same one shown on Fig.12. The intensity of almost all lines is decreased by 2.1 times.

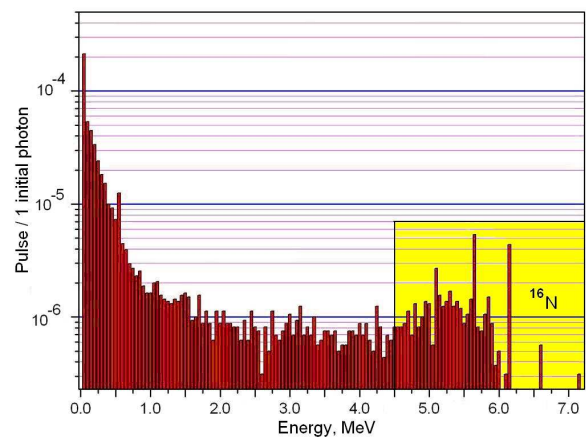


Fig.12. Absorbed energy distribution (response function) per 1 photon in the detector without collimator

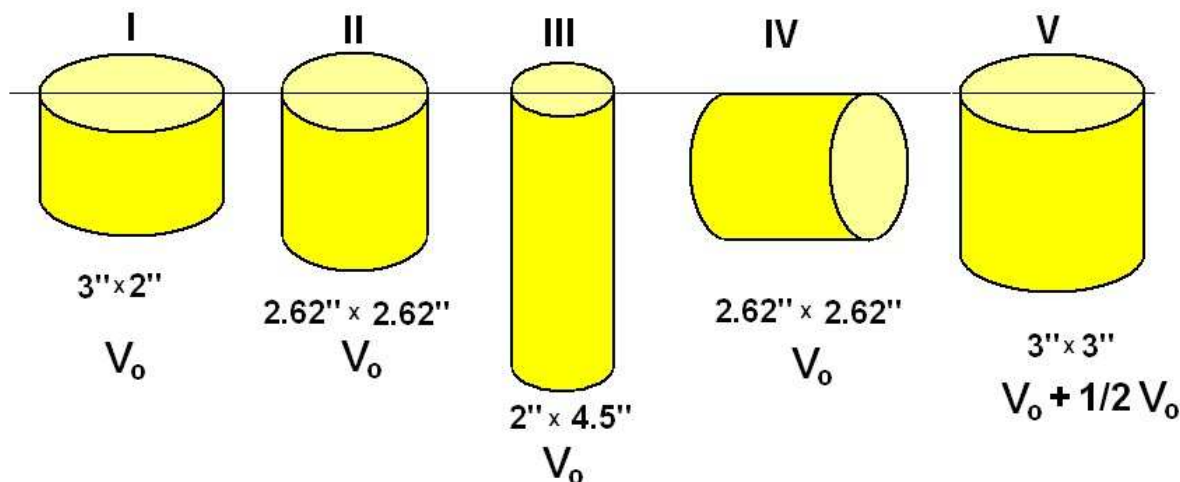


Fig.13. The cylindrical detectors based on a crystal NaI geometrical parameters variants

If we fix the initial volume V_0 in a form of a cylinder 3" diameter and a height of 2" we can propose several variants of detectors, that are shown in Fig. 13. ^{16}N Detection efficiency for variants of detectors II-IV insignificantly differ from the original version I and is shown in the table 4 below. Increasing the detector volume (with fixed base area) due to the height of the cylindrical crystal leads to increasing of the N_{eff} by a greater amount than the volume increase. The volume increased 1.5 times, and the efficiency increased 1.65 times. This was due to the fact that apart from increasing the length of the interaction of γ -ray, the lateral surface on which the photons can fall increased too. Note, that in the distribution of the absorbed energy (response function) significantly increased the number of absorbed photons in the energy range of 4.5...7.2 MeV compared to the number of absorbed photons with lower energies.

Table 4. Detection efficiency of nitrogen 16 for different variants of detectors

Variant Number	I	II	III	IV	V
$N_{eff} \times 10^5$	5.7	5.13	5.53	6.09	9.6

If the detector is in a protective casing (collimator) made of lead, an increase of N_{eff} for version V is somewhat less ≈ 1.45 . As the data on Fig. 11 shows, further increasing the thickness of the detector is ineffective. If necessary, the ^{16}N detection efficiency increase should be performed through increasing the diameter of the detector. This will lead to increasing the efficiency of detection that is proportional to the detector area growth.

6. CONCLUSIONS

The research of nitrogen 16 registration efficiency in the steam-line of WWER-1000 reactor has been performed. Using the method of volumetric integration of point sources the optimal placement of the detection system respectively to the steam-line was chosen. Simulation of radiation transport with the Monte-Carlo method (in packages MCNP and PENE-

LOPE) from the volume of steam-line to the scintillation detector was made. The technique designed to speed up the calculations significantly due to increasing the number of "virtual detectors" placed around the emitting steam was developed. The change in the spectral composition of ^{16}N radiation after the passage of steam-line steel walls and in the detector crystal NaI was estimated. The dependence of NaI detector thickness on the number of absorbed photons - deposited energy (the response function) in the energy range 4.5...7.2 MeV characterizing the presence of ^{16}N was studied. Variants of cylindrical detectors (constant volume) with different ratios of diameter to height and their placement relative to steam were investigated. It is shown that, when it is possible to increase the detector volume the thickness of the detector should be limited to about 3 inches. If necessary, increase of the ^{16}N detection efficiency can be performed through increasing the diameter of the detector.

Acknowledgements

We would like to thanks S.A. Pismenetskiy (Kharkiv National University, Kharkov, Ukraine) for his help and guidance in this research.

References

1. A.S. Kazimirov, G.F. Kazimirova, L.B. Martynjuk, S.M. Ievlev, E.V. Chernyj. Scintilljacionnye detektory v spektrometricheskij sistemah radiacionnoj bezopasnosti AJeS, jekologicheskogo i radiacionnogo kontrolja i monitoringa *ISMART-2012*, g. Dubna, Nauchno-proizvodstvennoe predprijatje "Atom-KompleksPrilad". 2012, 493 p (in Russian).
2. Firma RISTEC (in Russian) <http://www.ristec.ru/nuclear/>
3. MIRION TECHNOLOGIES <http://www.mgpi.de/die-mirion-gruppe/>

4. Evaluated Nuclear Data File (ENDF) Database Version of September 17, 2012
<http://www-nds.iaea.org/exfor/endl.htm>
5. S.B.Ludwig, J.P.Renier. *Standard- and Extended-Burnup PWR and BWR Reactor Models for the ORIGEN2 Computer Code*, ORNL/TM-11018, (December 1989).
6. B.E.Watt. Energy spectrum of neutrons from thermal fission of ^{235}U *Phys.Rev.* 1952, v. 87, N.6, p. 1037.
7. A.D.Galanin. *Vvedenie v teoriju jadernyh reaktorov na teplovyh nejtronah. 2-e izd.* M: "Jenergoatomizdat", 1990 (in Russian).
8. V.M.Kolobashkin, et. al. *Radiacionnye karakteristiki obluchennogo jadernogo topliva.*, M: "Jenergoatomizdat", 1983 (in Russian).
9. A.I.Kirjushin, E.F.Shlokin. *Osnovy proektirovaniya reaktornyh ustanovok*, M: "Jenergoatomizdat", 1991. 264 p. (in Russian).
10. J. Baro, J. Sempau, F. Salvat, J. Fernandez-Varea. PENELOPE: an algorithm for Monte Carlo simulation of the penetration and energy loss of electrons and positrons in matter // *Nucl. Instr. and Meth.* 1995, v. B100, p. 31-46.
11. MCNP - A General Monte Carlo N-Particle Transport Code, Version 5, Volume I: "Overview and Theory" *LA-UR-03-1987*, April 26, 2003.
12. *Rukovodstvo po radiacionnoj zashhite dlja inzhenerov.* / Pod red. D.L. Brodera i dr. M: "Atomizdat", v. 2, 1972, 288 p.(in Russian).
13. S.A.Pis'meneckij, V.G.Rudychev, Y.V.Rudychev, O.K.Tjutjunik. Analiz vneshnego izlucheniya cilindricheskoj emkosti s RAO // *Visnik Harkivs'kogo nacional'nogo universitetu im. V.N.Karazina.* N808. Ser. "Fizichna jadra, chastinki, polja", 2008, Harkiv, v.2(38), p. 53-60 (in Russian).
14. M.E.Globus, B.V.Grinev, *Neorganicheskie scintilljatory. Novye i tradicionnye materialy.* H: "Akta", p.2000-408 (in Russian).
15. Ljuk K.L. Juan, Vu Czjan'-Sjun. *Metody izmereniya osnovnyh velichin jadernoj fiziki.* M: "Mir", 1964 (in Russian).
16. D.W.O.Rogers and A.F.Belajew. *Monte Carlo Techniques of Electron and Photon Transport for Radiation Dosimetry.* Chapt.5, v.III of The Dosimetry of Ionizing Radiation / Ed.Kenneth R.Kase, et al. (Academic Press, 1990).

ОПТИМИЗАЦИЯ ДЕТЕКТИРУЮЩЕЙ СИСТЕМЫ ДЛЯ РЕГИСТРАЦИИ ^{16}N ПРИ ПРОТЕЧКАХ ТЕПЛОНОСИТЕЛЯ В ПАРОГЕНЕРАТОРЕ РЕАКТОРА ВВЭР-1000

В.Г. Рудычев, Е.В. Рудычев, Н.А. Азаренков, А.Ю. Бондарь

Одним из методов контроля протечек теплоносителя из 1-го во 2-й контур в парогенераторе реактора ВВЭР-1000 является измерение активности изотопа ^{16}N . Целью настоящей работы является оптимизация характеристик и размещения детекторов с кристаллами NaI(Tl). Методом Монте-Карло (в пакетах MCNP и PENELOPE) смоделирован транспорт излучения из объема паропровода в детектор. Разработана методика ускорения расчетов за счет увеличения количества "виртуальных детекторов", размещенных вокруг излучающего паропровода. Выполнено исследование влияния толщины детектора из NaI на количество поглощенных фотонов, характеризующих наличие ^{16}N – функция отклика детектора. Исследованы варианты цилиндрических детекторов постоянного объема с различными отношениями диаметра к высоте и оптимизировано их размещение относительно паропровода.

ОПТИМІЗАЦІЯ ДЕТЕКТУЮЩЕЙ СИСТЕМИ ДЛЯ РЕГИСТРАЦІЇ ^{16}N ПРИ ПРОТЕКАННІ ТЕПЛОНОСІЯ У ПАРОГЕНЕРАТОРІ РЕАКТОРА ВВЕР-1000

В.Г. Рудичев, Є.В. Рудичев, М.О. Азаренков, А.Ю. Бондар

Одним з методів контролю протікання теплоносія з 1-го у 2-й контур в парогенераторі реактора ВВЕР-1000 є вимірювання активності ізотопу ^{16}N . Метою цієї роботи є оптимізація характеристик та розташування детекторів з кристалами NaI(Tl). Методом Монте-Карло (у пакетах MCNP та PENELOPE) проведено моделювання транспорту випромінювання з об'єму паропроводу у детектор. Розроблена методика пришвидчення розрахунків за рахунок збільшення кількості "виртуальних детекторів", що розташовані навколо випромінюючого паропровода. Виконано дослідження впливу товщини детектора з NaI на кількість фотонів, що поглинаються, які характеризують наявність ^{16}N – функція відгуку детектора. Досліджені варіанти циліндричних детекторів постійного об'єму з різними відношеннями діаметру до висоти та оптимізовано їх розташування відносно паропроводу.